HEFAT2014
10th International Conference on Heat Transfer, Fluid Mechanics and Thermodynamics
14 – 16 July 2014
Orlando, Florida

NUMERICAL SIMULATION OF THREE-DIMENSIONAL NATURAL CONVECTION IN A CUBOID BOX CONTAINING HEAT GENERATING POROUS MEDIUM

A. K. Mishra, S. Kumar, R.V. Sharma*
*Author for correspondence
Department of Mechanical Engineering
NIT Jamshedpur-831013
India
E-mail: rvsharma.me@nitjsr.ac.in

ABSTRACT

The present numerical study presents results of steady three-dimensional natural convection in a cuboid box filled with fluid saturated porous medium. The porous medium is heated using uniform heat generation source. All six faces are subjected to isothermal condition. Darcy flow model has been employed. Governing equations have been numerically solved using Successive Accelerated Replacement Scheme. Maximum temperature and its location have been determined for wide range of parameters i.e. Rayleigh number, horizontal and vertical aspect ratios. As Rayleigh number increases, the value of maximum temperature decreases and its position shifts upward along mid vertical axis. There is significant effect of Rayleigh number and aspect ratios on flow and temperature fields.

INTRODUCTION

Studies on natural convection in porous media have practical applications of considerable importance in many engineering fields, such as storage of agricultural and food products, extraction of geothermal energy, underground disposal of nuclear waste material, pebble bed nuclear reactors, enhanced recovery of oil or gas by thermal methods, matrix heat exchangers, high performance insulation for cryogenic containers. The combination of natural convection in porous media with internal heat generation is interesting in view of applications to the above practical cases.

The onset of natural convection in horizontal infinite porous layer with internal heat generation has been studied by Gasser and Kazimi [1], Tveitereid [2] and Nouri-Borujerdi et al. [3]. Haajizadeh [4] studied steady natural convection inside a rectangular porous enclosure with uniform internal heat generation and cooling from the side walls. Prasad [5] studied thermal convection in a rectangular cavity filled with a heat generating, Darcy porous medium. Das and Sahoo [6] analyzed pressure-velocity solution of natural convection for fluid saturated heat generating porous medium in a square enclosure employing Brinkman extended Darcy flow model. Krishna et al. [7] studied natural convection in a two-dimensional square cavity containing hydro dynamically and thermally anisotropic porous medium with internal heat generation.

Studies on three-dimensional natural convection in porous media with internal heat generation are limited. Beukema et al. [8] developed a model for three-dimensional natural convection in a confined porous medium with internal heat generation. Experiments were performed on cooling the model material, representing agricultural products at different rates of heat generation in a closed container with isothermal walls. Compared to conduction only, natural convection accelerated cooling, resulting in lower average temperature from centre of the container upwards. Suresh et al. [9] studied three-dimensional natural convection in anisotropic heat generating porous medium enclosed inside a rectangular cavity.

The present numerical study investigates steady three-dimensional natural convection in a cuboid box with isothermal walls filled with heat generating porous medium. The effect of parameters like modified Rayleigh number (Ra), vertical aspect ratio (A_y) and horizontal aspect ratio (A_z) on the flow and temperature fields have been examined.

NOMENCLATURE

A_y	[-]	Vertical aspect ratio
A_z	[-]	Horizontal aspect ratio
B	[m]	Breadth in z-direction
Da	[-]	Darcy number
g	[m/s^2]	Acceleration due to gravity
H	[m]	Height in y-direction
K	[m^2]	Permeability of porous medium
k	[W/m K]	Thermal conductivity
L	[m]	Length in x-direction
P	[-]	Non-dimensional pressure
p	[N/m^2]	Fluid pressure
$\dot{q}$	[W/m^3]	Internal heat generation rate
Ra	[-]	Rayleigh number
T	[K]	Temperature of porous medium
U, V, W	[-]	Dimensionless Velocity components
u, v, w	[m/s]	Fluid velocity in x, y, z directions
X, Y, Z	[-]	Dimensionless Co-ordinate distances
x, y, z	[m]	Co-ordinates in dimensional form

Greek symbols

α	[m^2/s]	Effective thermal diffusivity
β	[K^{-1}]	Thermal expansion coefficient of fluid
ε	[-]	Error tolerance limit

μ	[N-s/m^2]	Dynamic viscosity of fluid
ν	[m^2/s]	Kinematic viscosity of fluid
ρ	[kg/m^3]	Fluid density
$\bar{\rho}$	[-]	Dimensionless fluid density
$\vec{\Psi}$	[-]	Dimensionless vector potential
θ	[-]	Dimensionless temperature
ω	[-]	Acceleration factor

Subscripts

c cold

MATHEMATICAL FORMULATION

The mathematical model for a steady three-dimensional natural convection in a cuboid box filled with heat generating porous medium is presented. All surfaces are assumed to be at constant temperature, T_c. The Physical model and co-ordinate system is shown in Figure 1. The flow is governed by Darcy law. Boussinesq approximation is valid. The fluid and solid matrix are in thermal equilibrium. Viscous dissipation and pressure work are negligible. Porous medium is isotropic and homogeneous.

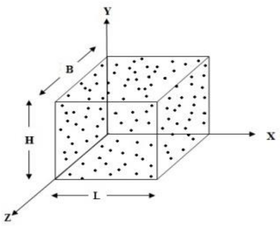

Figure 1 Physical model and co-ordinate system

With above assumptions, the governing equations are given as,

$$\frac{\partial u}{\partial x}+\frac{\partial v}{\partial y}+\frac{\partial w}{\partial z}=0 \quad (1)$$

$$\frac{\mu u}{K}=-\frac{\partial p}{\partial x} \quad (2)$$

$$\frac{\mu v}{K}=-\frac{\partial p}{\partial y}-\rho g \quad (3)$$

$$\frac{\mu w}{K}=-\frac{\partial p}{\partial z} \quad (4)$$

$$\rho c_p\left(u\frac{\partial T}{\partial x}+v\frac{\partial T}{\partial y}+w\frac{\partial T}{\partial z}\right)=k\left(\frac{\partial^2 T}{\partial x^2}+\frac{\partial^2 T}{\partial y^2}+\frac{\partial^2 T}{\partial z^2}\right)+\dot{q} \quad (5)$$

$$\rho=\rho_c\,[1-\beta\,(T-T_c)] \quad (6)$$

Solutions to Equations (1) to (6) are sought subject to following boundary conditions:

$$u=0,\quad T=T_c,\quad \text{at } x=0, L$$

$$v=0,\quad T=T_c,\quad \text{at } y=0, H$$

$$w=0,\quad T=T_c,\quad \text{at } z=0, B \quad (7)$$

Governing equations are rendered dimensionless introducing the following dimensionless variables:

$$X=\frac{x}{L},\quad Y=\frac{y}{L},\quad Z=\frac{z}{L},$$
$$U=\frac{u}{\alpha/L},\quad V=\frac{v}{\alpha/L},\quad W=\frac{w}{\alpha/L}$$

$$\theta=\frac{T-T_c}{qL^2/k}\qquad P=\frac{p}{\mu\alpha/K} \quad (8)$$

The Vector potential, $\vec{\Psi}$ which satisfies the continuity equation, is related to the velocity vector, $\vec{V}$ by

$$\vec{V}=\nabla\times\vec{\Psi} \quad (9)$$

Since $\nabla.\vec{V}=0$, the modified vector potential is also solenoidal over the domain considered. Thus,

$$\nabla.\vec{\Psi}=0 \quad (10)$$

Governing equations in non-dimensional form are transformed using vector potential formulation to eliminate pressure by taking curl of the momentum equations. The corresponding governing equations become:

$$\frac{\partial^2\psi_X}{\partial X^2}+\frac{\partial^2\psi_X}{\partial Y^2}+\frac{\partial^2\psi_X}{\partial Z^2}=-R_a\,\frac{\partial\theta}{\partial Z} \quad (11)$$

$$\frac{\partial^2\psi_Y}{\partial X^2}+\frac{\partial^2\psi_Y}{\partial Y^2}+\frac{\partial^2\psi_Y}{\partial Z^2}=0 \quad (12)$$

$$\frac{\partial^2\psi_Z}{\partial X^2}+\frac{\partial^2\psi_Z}{\partial Y^2}+\frac{\partial^2\psi_Z}{\partial Z^2}=R_a\,\frac{\partial\theta}{\partial Z} \quad (13)$$

$$\left(\frac{\partial\Psi_Z}{\partial Y}-\frac{\partial\Psi_Y}{\partial Z}\right)\frac{\partial\theta}{\partial X}+\left(\frac{\partial\Psi_X}{\partial Z}-\frac{\partial\Psi_Z}{\partial X}\right)\frac{\partial\theta}{\partial Y}+\left(\frac{\partial\Psi_Y}{\partial x}-\frac{\partial\Psi_X}{\partial Y}\right)\frac{\partial\theta}{\partial Z}=\frac{\partial^2\theta}{\partial X^2}+\frac{\partial^2\theta}{\partial Y^2}+\frac{\partial^2\theta}{\partial Z^2}+1 \quad (14)$$

The boundary conditions on vector potential ($\vec{\Psi}$) as given by Hirasaki and Hellums (1968):

$$\frac{\partial\Psi_X}{\partial X}=\Psi_Y=\Psi_z=0,\quad at\ X=0,1$$

$$\frac{\partial\Psi_Y}{\partial Y}=\Psi_Z=\Psi_X=0,\quad at\ Y=0, A_y$$

$$\frac{\partial\Psi_Z}{\partial Z}=\Psi_X=\Psi_Y=0,\quad at\ Z=0, A_z \quad (15)$$

The boundary condition on temperature (θ) is given by

$$\theta=0,\quad at\ X=0,1$$

$$\theta=0,\quad at\ Y=0, A_y$$

$$\theta=0,\quad at\ Z=0, A_z \quad (16)$$

The dimensionless parameters i.e. modified Rayleigh number (Ra), vertical aspect ratio (A_y) and horizontal aspect ratio (A_z) appearing in above equations are defined as,

$$Ra=\frac{K\dot{q}L^3 g\beta}{\nu\,\alpha\,k} \quad (17)$$

$$A_y=\frac{H}{L} \quad (18)$$

$$A_z=\frac{B}{L} \quad (19)$$

NUMERICAL SCHEME

Numerical solutions to the governing equations have been obtained by employing Successive Accelerated Replacement (SAR) Scheme. Chandra and Satyamurty [10] and Sangita et al. [11] have demonstrated the applicability of the SAR scheme for solving system of partial differential equations in the study of two-dimensional natural convection heat transfer in porous media. The same scheme has been extended to solve three-dimensional natural convection in porous media.

The basic philosophy of this scheme is to guess profile for each variable that satisfies the boundary conditions. The equations are transformed into finite difference employing central differencing scheme. Let governing equation of variable Φ is given by $\widetilde{\Phi}_{i,j,k}$, at any mesh point i, j, k corresponding to $X, Y$and Z position. The error arising out of the guessed profile is evaluated. Let the error arising in equation at (i, j, k) and the n^{th} iteration be $\widetilde{\Phi}_{i,j,k}^{n}$,. The $(n + 1)^{th}$ approximation to the variable Φ is given as,

$$\Phi_{i,j,k}{}^{n+1} = \Phi_{i,j,k}{}^{n} - \omega \frac{\widetilde{\Phi}_{i,j,k}{}^{n}}{\partial \widetilde{\Phi}_{i,j,k}{}^{n} / \partial \Phi_{i,j,k}} \qquad (20)$$

ω is the acceleration factor which varies from 0 to 2.The procedure of correcting the variable at every mesh point is repeated until a set of convergence criteria is satisfied. The criterion is given by,

$$\frac{\sum_i \sum_j \sum_k |\Phi_{i,j,k}{}^{n+1} - \Phi_{i,j,k}{}^{n}|}{\sum_i \sum_j \sum_k |\Phi_{i,j,k}{}^{n+1}|} \leq \varepsilon \qquad (21)$$

ε is the error tolerance limit. The feature of using the corrected value of the variable immediately upon becoming available is inherent in this method.

RESULTS AND DISCUSSION

Numerical code based on SAR Scheme has been developed in MSDEV-FORTRAN. Grid sensitivity tests have been carried and results are given in Table 1. A grid size of 31×31×31 has been considered as optimum. Error tolerance limit (ε) value of 10^{-4} has been taken for all computations. Acceleration factor (w) value of 0.5 (under relaxation) for Ra>1000 and 1.5 (over relaxation) for Ra<1000 has been employed.

For validation of the present mathematical model and numerical scheme, maximum temperature experimentally measured by Beukema et al. [8] for various heat generation rates have been compared with computed results in the present study and are given in Table 2. The results are in agreement which validates the present mathematical model and the numerical scheme.

Table 1: Grid sensitivity test for Ra=1000, A_y= A_z=1.0

Grid size	Maximum temperature, θ_{max}
$16 \times 16 \times 16$	0.04780
$31 \times 31 \times 31$	0.04801
$61 \times 61 \times 61$	0.04837
$121 \times 121 \times 121$	0.04822

Flow and Temperature Fields

Figures 2-4 depict flow fields in terms of iso-vector potential lines ($\overrightarrow{\psi_x}$) at X=0.5 for Ra=100, 1000 and 10000. It can be observed that as Rayleigh number increases, bi-cellular flow becomes more dominant. Figures 5-7 depict temperature fields in terms of isotherms at X=0.5 for Ra=100, 1000 and 10000. It can be observed that as Rayleigh number increases, isotherms become finer near the top surface indicating more heat transfer from the top face. Also, maximum temperature shifts upwards as Rayleigh number increases.

Table 2: Comparison of experimental results of Beukema et al. (1983) with the present computed maximum temperature (T_{max}) for Ay= 0.66 and A_z=1.0

Heat generation rate q (Wm^{-3})	Beukema et al. [8] T_{max} (^0C)	Present T_{max} (^0C)	% error
15	20.62	20.58	0.19
28	21.65	21.56	0.42
60	23.92	23.80	0.50
115	27.39	26.80	2.15
171	30.74	29.26	4.81
235	33.88	31.80	6.14

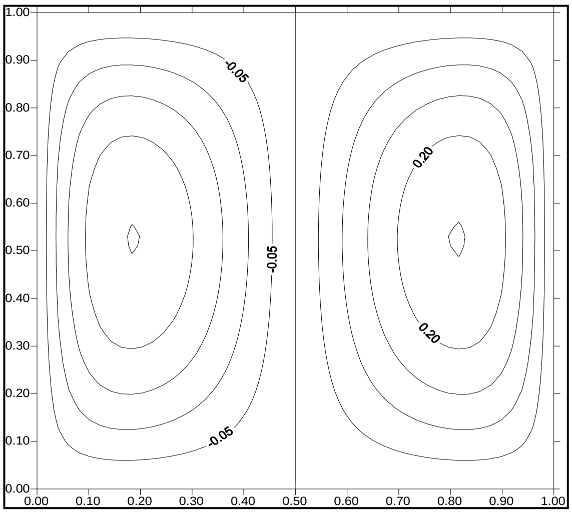

Figure 2 Plot of iso-vector potential lines ($\overrightarrow{\psi_x}$) at X=0.5 for Ra=100 and A_y=A_z=1

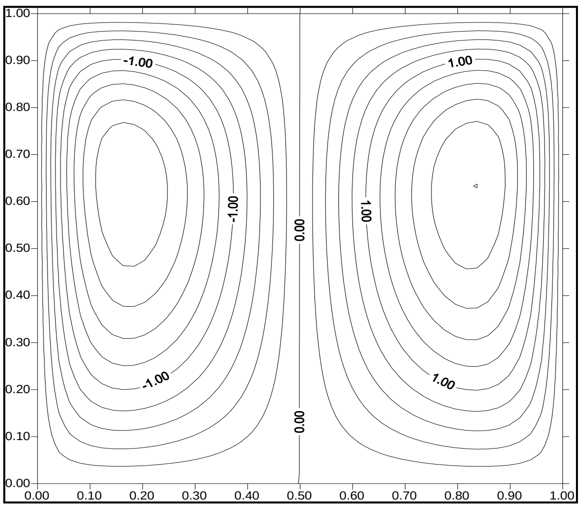

Figure 3 Plot of iso-vector potential lines ($\overrightarrow{\psi_x}$) at X=0.5 for Ra=1000 and A_y=A_z=1

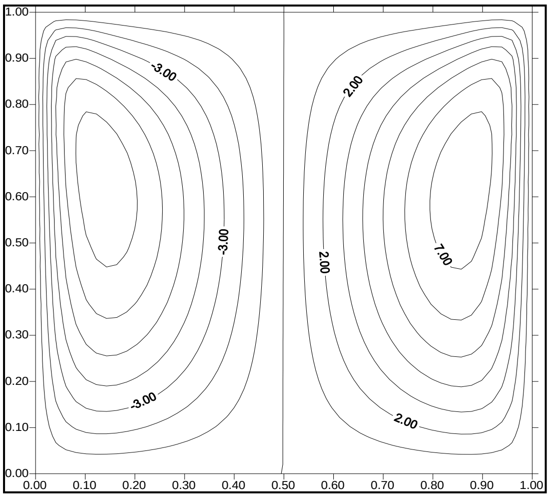

Figure 4 Plot of iso-vector potential lines ($\overrightarrow{\psi_x}$) at X=0.5 for Ra=10000 and A_y=A_z=1

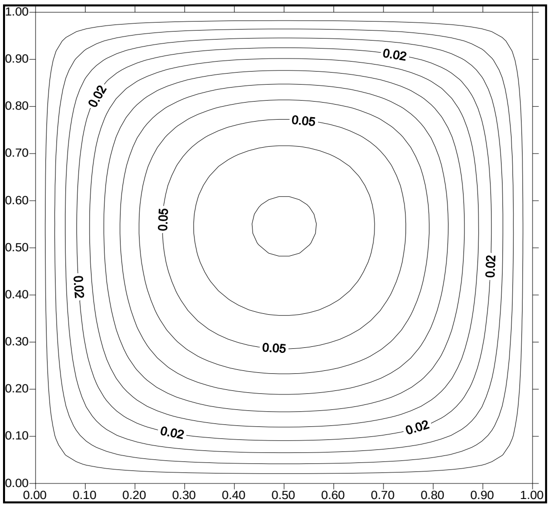

Figure 5 Plot of isotherms at X=0.5 for Ra=100 and A_y=A_z=1

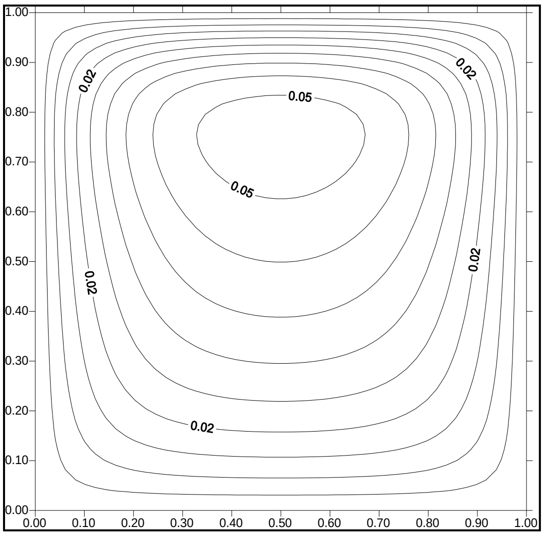

Figure 6 Plot of isotherms at X=0.5 for Ra=1000 and A_y=A_z=1

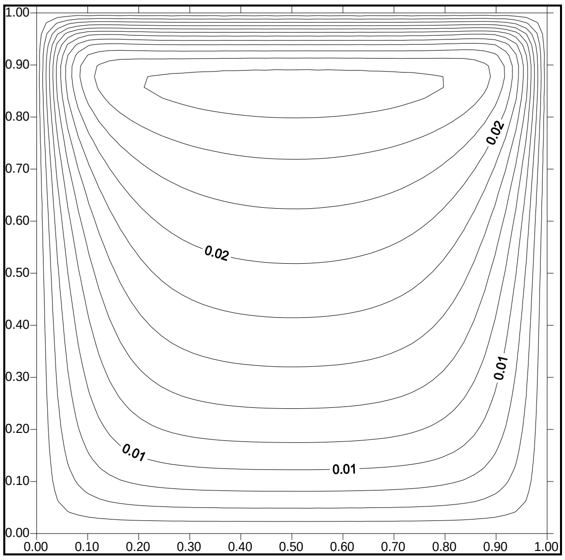

Figure 7 Plot of isotherms at X=0.5 for Ra=10000 and A_y=A_z=1

Maximum Temperature and its Location

Variation of maximum temperature with Rayleigh number at different aspect ratios is shown in Figure 8. It can be seen that as Rayleigh number increases, value of maximum temperature decreases. This is because as Rayleigh number increases flow of fluid inside the porous box increases which increase heat transfer from the wall thereby lowering the maximum temperature in the box. For a given Rayleigh number, as vertical aspect ratio increases maximum temperature increases but it decreases with increase in horizontal aspect ratio. As vertical aspect ratio increases fluid has to overcome gravity force which slows down flow velocity in vertical direction thereby lowers heat transfer and maximum temperature increases.

Variation of temperature along central Y-axis is shown in Figure 9 for Ra=0 (pure conduction) and Ra=100, 1000 and 10000. It can be noted that for pure conduction, maximum temperature is located at the center (Y=0.5) i.e center the box. As convection increases, the value of maximum temperature decreases and the location of maximum temperature shift upwards along central Y-axis.

CONCLUSIONS

The present study presents numerical results for mathematical model of steady three- dimensional natural convection in a rectangular box filled with heat generating porous medium employing Darcy flow model. There is significant effect of Rayleigh number on flow and temperature fields. As Rayleigh number increases, the maximum temperature in the porous box decreases. The position of maximum temperature shifts upward with increase in Rayleigh number.

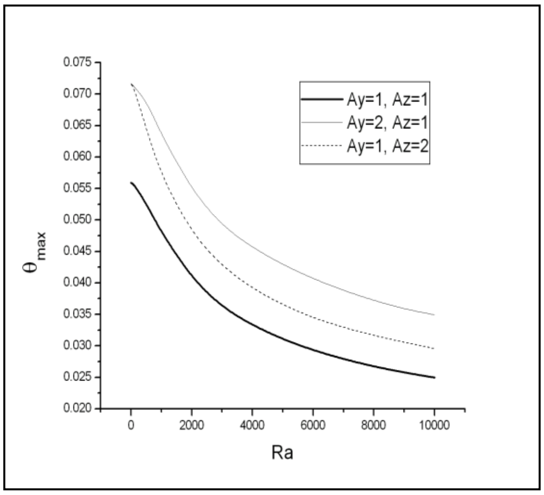

Figure 8 Variation of maximum temperature with Rayleigh number

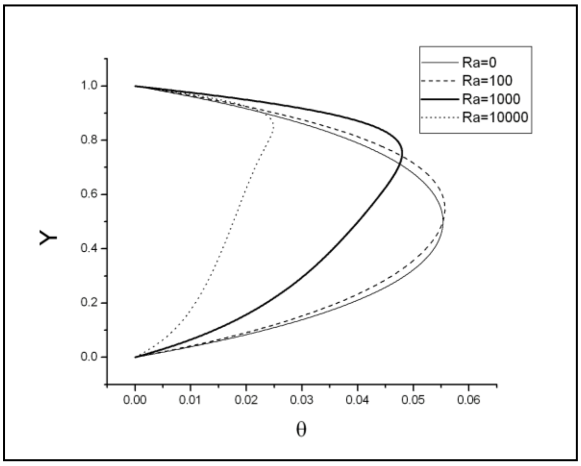

Figure 9 Variation of temperature along central Y-axis

REFERENCES

1. Gasser, R.D. and Kazimi, M.S., Onset of convection in a porous medium with internal heat generation, J. Heat Transfer, vol.98, 1976, pp.49-54.
2. Tveitereid, M., Thermal convection in a horizontal porous layer with internal heat sources, Int. J. Heat Mass Transfer, vol.20, 1977, pp.1045-1050.
3. Nouri-Borujerdi, A., Noghrehabadi A.R., and Rees D.A.S., Influence of Darcy number on the onset of convection in a porous layer with a uniform heat source, International Journal of Thermal Sciences, vol.47, 2008, pp.1020-1025.
4. Haajizadeh, M., Ozguc, A. F. and Tien, C. L., Natural convection in a vertical porous enclosure with internal heat generation, International Journal of Heat and Mass Transfer, vol.27, 1984, pp.1893-1902.
5. Prasad, V., Thermal convection in a rectangular cavity filled with a heat generating, Darcy porous medium, ASME J. Heat Transfer, vol.109,1987,pp. 697-703.
6. Das, S. and Sahoo, R.K., Effects of Darcy, Fluid Rayleigh and heat generation parameters on natural convection in a porous square enclosure: A Brinkman-extended Darcy model, Int. Comm. Heat Mass Transfer, vol.26, pp.569-578.
7. Krishna, D. J., Basak, T. and Das, S. K., Natural convection in a heat generating hydrodynamically and thermally anisotropic non-Darcy porous medium, International Journal of Heat and Mass Transfer, vol.51, 2008, vol.4691-1902
8. Beukema, K. J., Bruin, S. and Schenk, J., Three-dimensional natural convection in a confined porous medium with internal heat generation, International Journal of Heat and Mass Transfer, vol.26, 1983, pp.451-458.
9. Suresh, C. S. Y., Krishna, Y. V, Sundararajan, T. and Das, S. K., Numerical simulation of three-dimensional natural convection inside a heat generating anisotropic porous medium, Heat and Mass Transfer, vol.41, 2005, pp.799-809.
10. Chandra P. and Satyamurty V.V., Non-Darcian and anisotropic effects on free convection in a porous Enclosure, Transport in Porous Media, vol. 90, 2011, pp.301–320.
11. Sangita, Sinha M. K. and Sharma R. V., Natural convection in a spherical porous annulus: The Brinkman extended Darcy flow model, Transport in Porous Media vol.100, 2013, pp.321–335.
12. Nield D.A. and Bejan, A., Convection in porous media, 3rd edition, Springer, New York, 2006.